Annual Review of Chemical and Biomolecular Engineering

Scale-Up of Photochemical Reactions: Transitioning from Lab Scale to Industrial Production

Stefan D.A. Zondag,[1,*] Daniele Mazzarella,[1,2,*] and Timothy Noël[1]

[1]Flow Chemistry Group, van 't Hoff Institute for Molecular Sciences (HIMS), University of Amsterdam, Amsterdam, The Netherlands; email: t.noel@uva.nl

[2]Department of Chemical Sciences, University of Padova, Padova, Italy

https://doi.org/10.1146/annurev-chembioeng-101121-074313

*These authors contributed equally to this article

Keywords

scale-up, photochemistry, photocatalysis, numbering up, sizing up, flow chemistry

Abstract

In the past two decades, we have witnessed a rapid emergence of new and powerful photochemical and photocatalytic synthetic methods. Although these methods have been used mostly on a small scale, there is a growing need for efficient scale-up of photochemistry in the chemical industry. This review summarizes and contextualizes the advancements made in the past decade regarding the scale-up of photo-mediated synthetic transformations. Simple scale-up concepts and important fundamental photochemical laws have been provided along with a discussion concerning suitable reactor designs that should facilitate scale-up of this challenging class of organic reactions.

INTRODUCTION

In the past two decades, we have witnessed a new wave in the field of synthetic organic chemistry: Increasing reports of synthetic protocols rely on the use of photons to produce value-added molecules, including pharmaceuticals, agrochemicals, and materials (1). The reason for such a widespread interest in photochemistry and photocatalysis lies in the provided new synthetic opportunities, as well as the associated mild reaction conditions, such as the use of visible light, the absence of hazardous redox reagents, and room-temperature reaction conditions.

Photochemistry is the branch of chemistry concerned with the chemical effects of light (2, 3). The interaction between photons and molecules generally results in a transition of one electron from the highest occupied molecular orbital (HOMO) to the lowest unoccupied molecular orbital (LUMO). This affords electronically excited-state molecules, which are totally different reactive species compared to their ground-state analogs (4). These excited intermediates possess different electronic distributions, energies, and lifetimes and can be engaged in various synthetic processes, thus providing access to products that are otherwise challenging to make, e.g., cyclobutanes via [2 + 2] cycloadditions (5). Unfortunately, this direct activation of organic molecules is limited by the generally large HOMO–LUMO gap. As a consequence, dangerous, high-energy UV irradiation is required to access these excited states. Furthermore, organic molecules are generally characterized by a low molar attenuation coefficient, thus limiting the amount of light absorbed by the molecule at a given wavelength.

To tackle these issues, an alternative bimolecular strategy, called photocatalysis, has been developed. This approach relies on the use of photon-mediator compounds (e.g., transition-metal complexes, organic dyes, and polyoxometalate compounds). These compounds, which can absorb light in the near-UV or visible light range and possess high molar attenuation coefficients, can activate surrounding molecules mainly through three distinct mechanisms: electron transfer (6), energy transfer (7), and hydrogen atom transfer (8).

Both synthetic photochemistry and photocatalysis have enabled the exploration of new chemical space by fostering novel radical-generating strategies, thereby solving longstanding synthetic challenges. Indeed, the extremely mild conditions required for the production of these open-shell species has spurred the recent renaissance of radical chemistry (9). Moreover, the use of photons to drive chemical reactions can be considered green and sustainable, especially when compared to the need for high reaction temperatures or for stoichiometric amounts of radical-inducing agents for the conventional synthetic processes (10–12). This is reinforced by the fact that photocatalysts are generally used in very low catalytic amounts and can even activate C–H bonds within organic molecules (8), thus obviating the need for functionalized starting materials.

However, many of these new synthetic transformations are run solely on a small laboratory scale. This includes those examples carried out in the pharmaceutical and agrochemical industries, where photochemistry is used mainly for the small-scale, high-throughput preparation of active compounds (13). Indeed, the transition from small scale to larger processes on pilot and industrial scales remains challenging for photon-induced processes (14). Owing to photon transport limitations (i.e., attenuation effect), the typical scale-up strategy of dimension enlargement of the reactor vessel is not effective for photochemistry. The use of larger-diameter reactors would result in low penetration of the crucial irradiation, thus leading to longer reaction times and possible by-product formation. In contrast, flow chemistry (15) has proven to be a powerful ally to scale such processes (16, 17). The main reason can be found in the reduced optical path and its ability to increase the throughput via continuous introduction of starting materials.

This review summarizes the different scale-up strategies that can be used to scale photochemical reaction conditions. As shown herein, in the past few years, the academic and industrial

communities have made huge technological strides toward realizing scale-up of this challenging activation mode. In all cases, the balanced combination of chemistry, reactor technology, and suitable light source is critical.

CONCEPTS OF SCALE-UP IN PHOTOCHEMISTRY

As recent developments in photochemistry indicate an apparent shift from batch to continuous flow, it is important to understand exactly why this shift is desired en route to larger-scale production. Even up to now, small-scale production is generally performed in batch. Major reasons for this focus on batch processing are the traditional practices in teaching and laboratory environments (with a focus on round-bottom flasks), a lack of in-depth knowledge of flow chemistry and chemical engineering, and most importantly the perceived limited necessity of flow chemistry in this small-scale setting. For small-scale production, batch operating parameters are often easily controlled and varied, and the produced quantities suffice for the intended purposes. However, when larger quantities are required, the scalability problems of batch photochemistry arise quickly, and at this stage flow chemistry cannot be ignored (18).

Notably, the use of micro- and milli-flow reactors can already improve productivity, safety of operation, and selectivity through enhanced mass and heat transfer on a small scale (19). Moreover, the continuous nature of flow reactors allows for consistent product quality and overall more sustainable operation and screening possibilities through process analytical technological capabilities compared to batch processes (20). There are several well-established strategies for scaling up micro- and milli-flow processes, as well as ongoing research efforts into solving remaining scalability issues (21–23). The common strategies to scale up reactor volume (V) can be divided into two main categories: numbering up and sizing up (**Figure 1**), both of which have been described in great detail elsewhere (21) but are summarized briefly here because of their importance to the scaling of photochemical processes. The scaled-up reactor volume can be approximated for tubular/capillary plug flow reactor (PFR) types using Equation 1:

$$V = \frac{\pi}{4} \cdot N \cdot L \cdot D^2, \qquad 1.$$

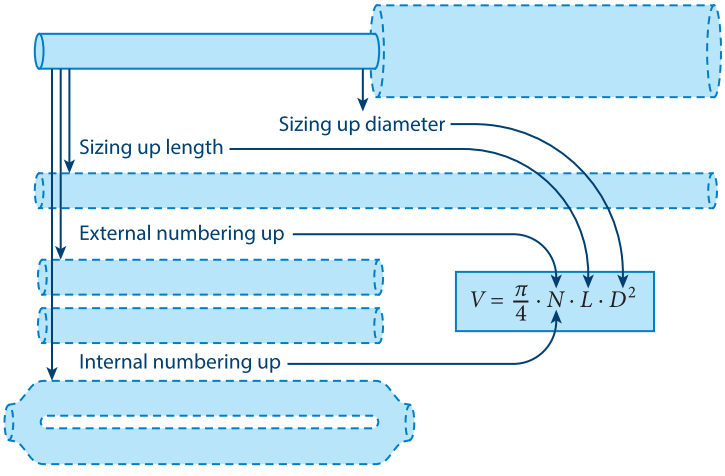

Figure 1

Visualization of scale-up strategies for capillary/tubular reactors.

where N, L, and D are the number of channels, channel length, and channel diameter, respectively. Simply put, the numbering-up strategy is concerned with increasing N, whereas sizing up revolves around enlarging the L and D terms. Often, a combination of both strategies is applied.

The numbering-up strategy is usually regarded as the simplest of the two because it involves multiplication of a system or setup to increase productivity any number of times. Simply copying an entire system (also called external numbering-up) ensures straightforward increased productivity, but the main downside to this approach is the high associated cost of multiplication. Internal numbering-up increases only the number of reactor units within the system (e.g., channels, microreactors). This can increase productivity without the additional costs for ancillary equipment (e.g., pumps, control units) but introduces a new challenge in the form of equal flow distribution (equipartitioning). Whereas external numbering-up can ensure identical operating parameters across the separate devices, the governing issue for internal numbering-up is that small pressure differences in the feeding or collection zones can cause maldistribution of the flow, resulting in different residence times experienced across the internally reproduced reactor units (24).

The second strategy, sizing up, makes use of dimension enlarging, whereby reactor channel diameters or lengths can be increased. Contrary to numbering-up, changing these parameters can strongly affect the processing effectiveness of a system, because it affects the hydrodynamic behavior and the mass-, heat-, and photon-transfer properties. Elongating reactor channels while maintaining identical residence times positively influences mixing and mass/heat transfer in the system but increases the pressure drop. In contrast, increasing the diameter can reduce the pressure drop but will diminish the advantages of micro- and millireactors, such as short diffusion lengths and isothermal operation due to a lower surface-to-volume ratio. However, there is an important reason that sizing up the diameter is an attractive approach: the quadratic relation between diameter and volume (e.g., doubling the diameter quadruples the available reactor volume). Consequently, many approaches are possible in sizing-up strategies, each with their own advantages and disadvantages, making the ideal scale-up approach dependent on case-by-case considerations.

When we shift the focus from general scale-up strategies to photochemical applications specifically, an additional factor must be considered, i.e., light irradiation. Similar to the well-known transport phenomena required for traditional chemical transformations, in photochemistry photon-transport phenomena must be taken into account. The overall effectiveness of photochemical transformations depends on the ability of photons to reach the reaction mixture and effectively contribute to these transformations. Therefore, an important aspect in scaling-up photochemistry is the quantification or reliable comparison of light irradiation between different setups and scales and an understanding of the underlying principles that govern photochemical reaction rates. A comprehensive overview of these fundamental laws and principles of photochemistry is given by Edwards and coauthors (25) and briefly summarized and visualized in **Table 1** and **Figure 2**.

All these fundamental laws simultaneously create an intricately defined system of considerations. To successfully carry out any photochemical transformation, the Grotthuss–Draper law highlights the importance of light source selection. Improper matching of the emitted wavelengths to the absorption spectrum of reaction media results in poor light absorption, which is the essential first step to any photochemical transformation.

Another important aspect in optimizing photochemical transformations derived from the Stark–Einstein law is the determination of the quantum yield. The quantum yield (φ) is defined as the number of formed molecules per number of absorbed photons. This quantity is generally between 0 and 1, given relaxation/quenching of the excited state can occur via multiple desirable and undesirable pathways. Of note, seemingly contradictory to the Stark–Einstein law, its value can exceed 1 for radical chain processes (27). Knowing the quantum yield of a certain photochemical

Table 1 A brief overview of the fundamental laws of photochemistry

1	Grotthuss–Draper law	For any photochemical transformation to take place, light must first be absorbed.
2	Stark–Einstein law	Often called the law of photochemical equivalence, this law states that one photon can solely activate a single molecule.
3	Bunsen–Roscoe law	According to this law, only the total supplied energy dose is significant for photochemical transformations. This energy dose is defined as the product of light intensity and irradiation time ($I \times t = \text{constant}$).
4	Inverse-square law	The light intensity originating from a light source is inversely proportional to the distance from the source squared.
5	Bouguer–Lambert–Beer law	This law relates the decrease in light intensity through a medium due to attenuation of light ($A = \varepsilon c l = \log_{10}\frac{I_0}{I} = -\log_{10} T$).

reaction can contribute not only to understanding the underlying mechanism but also to determining whether light irradiation and intensity should be key considerations moving forward. This light intensity reaching the reaction mixture depends heavily on the selected light source in terms of emission spectrum, distance from the reaction medium, attenuation through the medium, and initial light intensity at the source. The effective output of light sources can be characterized using integrating sphere measurements or chemical actinometry. Chemical actinometry makes use of a reaction with a known quantum yield to calculate the photon flux generated by the light source and also allows for determination of the quantum yields for other photochemical transformations (28, 29).

The Bunsen–Roscoe law highlights an interesting concept in photochemistry that is uniquely relevant for scale-up. The higher the light intensity is, the faster the reaction rates and the higher the throughput can be, thus enabling large-scale production. This is generally true and often results in the use of high-power light sources to realize the required shift from small-scale batch to

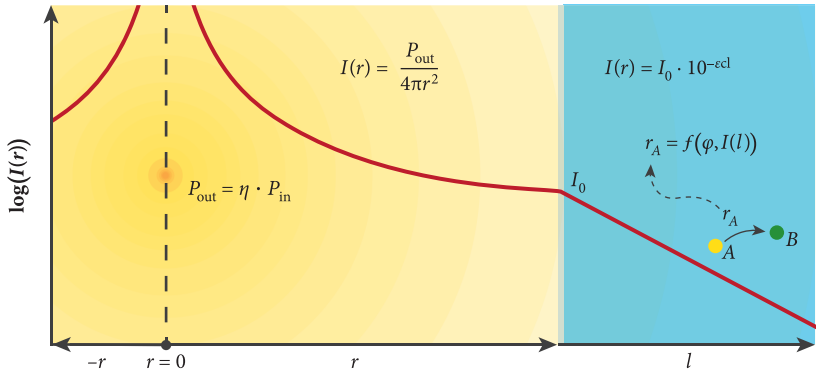

Figure 2

A qualitative and simplified visual representation of fundamental steps in a photochemical setup. A point source placed at $r = 0$ with input power P_{in}, efficiency η, and optical power P_{out} irradiates a sample. The light intensity, $I(r)$, indicated by the red curve, decreases according to the inverse-square law at increasing distance r away from the point source. The light reaches the sample with an intensity of I_0, and this intensity $I(l)$ decreases along the traveled path l within the sample according to the Bouguer–Lambert–Beer law, dependent on the molar attenuation coefficient ε of the absorbing species and its concentration c. The reaction rate r_A of a simple $A \rightarrow B$ transformation within the sample is governed by the quantum yield φ and the local absorption rate (26), which is in turn dependent on the local light intensity.

larger-scale flow setups. However, this law does not consider undesired sequential photochemical reactions, where local high-intensity light can result in by-product formation.

The inverse-square law makes use of the idea that the further the reactor is from a light source, the lower the intensity will be in the reaction mixture. The greater the distance, the more the radiant power is spread across an increasingly large surface. This is inversely proportional to the square of the distance, which translates to the conventional unit of light intensity in W/m^2. The example depicted in **Figure 2** uses an omnidirectional light source, which makes this surface equivalent to a perfect sphere. However, for focused/directional light sources (e.g., laser), this absolute intensity loss can be less extreme due to smaller equivalent irradiated surfaces.

Finally, the attenuation of light by a chemical species in solution as a function of the traveled path length is commonly described using the Bouguer–Lambert–Beer law. This dependence of received light intensity on the path length is what strongly affects the feasibility of reactor designs for scale-up. The conventional dimension-enlarging strategies significantly influence the irradiation homogeneity, where the highest intensities are found at the reactor walls and dark zones are encountered at the reactor center. The larger the reactor diameter, the larger the dark zone will become, which influences by-product formation, reaction times, and overall process control. This dimensional limitation can be considered the main reason for the interest in continuous-flow processes to scale up photochemical transformations. Notably, the small dimensions found in micro- and milli-flow reactors enable homogeneous irradiation across the entire reactor volume, thus ensuring that similar reaction kinetics are obtained.

Considering these laws and principles, several unique approaches can contribute to an overall understanding of what is important in scaling up. The Stark–Einstein law inspired the method of viewing photons as traceless reagents that require a certain stoichiometry and can therefore be expressed as a number of equivalents relative to the substrate (i.e., photon equivalents) (30). Chemical actinometry is often used to identify the role of photons in a system and can help identify what limits productivity. For instance, increasing reaction rates by intensifying light irradiation will reach a point where the reaction mixture is saturated with photons, and thus where focus should be turned toward enhancing other elementary steps, such as mass-transfer and reaction kinetics (31). Using these types of approaches in identifying which step in the overall system limits productivity can shift the primary focus of the scale-up strategy. Consequently, numerous photochemical reactors have been reported for scale-up, ranging in sizes, design principles, and application intent (32–34).

In general, scaling up photochemical systems is an intricate balance between light irradiation, the chemicals used, and reactor materials and geometry (35), resulting in trade-offs between kinetics, transport phenomena, and cost. To fully appreciate and grasp the essential factors of this field, an overview of some interesting developments and novel design efforts is discussed in the following sections.

RECENT ADVANCES AND WORK

In continuous-flow processing, tubular/capillary PFR-type reactors are frequently used to enable scale-up. A selected overview of some seminal works and recent advances in the field of scale-up is presented here, including some designs that deviate from this PFR-type standard to highlight the versatility and possibilities within the field.

Booker-Milburn and coworkers (36) detailed the design of a photochemical flow reactor capable of carrying out large-scale reactions (>500 grams per day) in a single pass. This reactor consists of fluorinated ethylenepropylene tubing [internal volume 210 mL, inner diameter (ID) 2.7 mm] coiled around a Vycor immersion well, irradiated from within the reactor assembly (**Figure 3*a***). The choice of material, for both the tubing and the glass reactor, is crucial to avoid absorption of

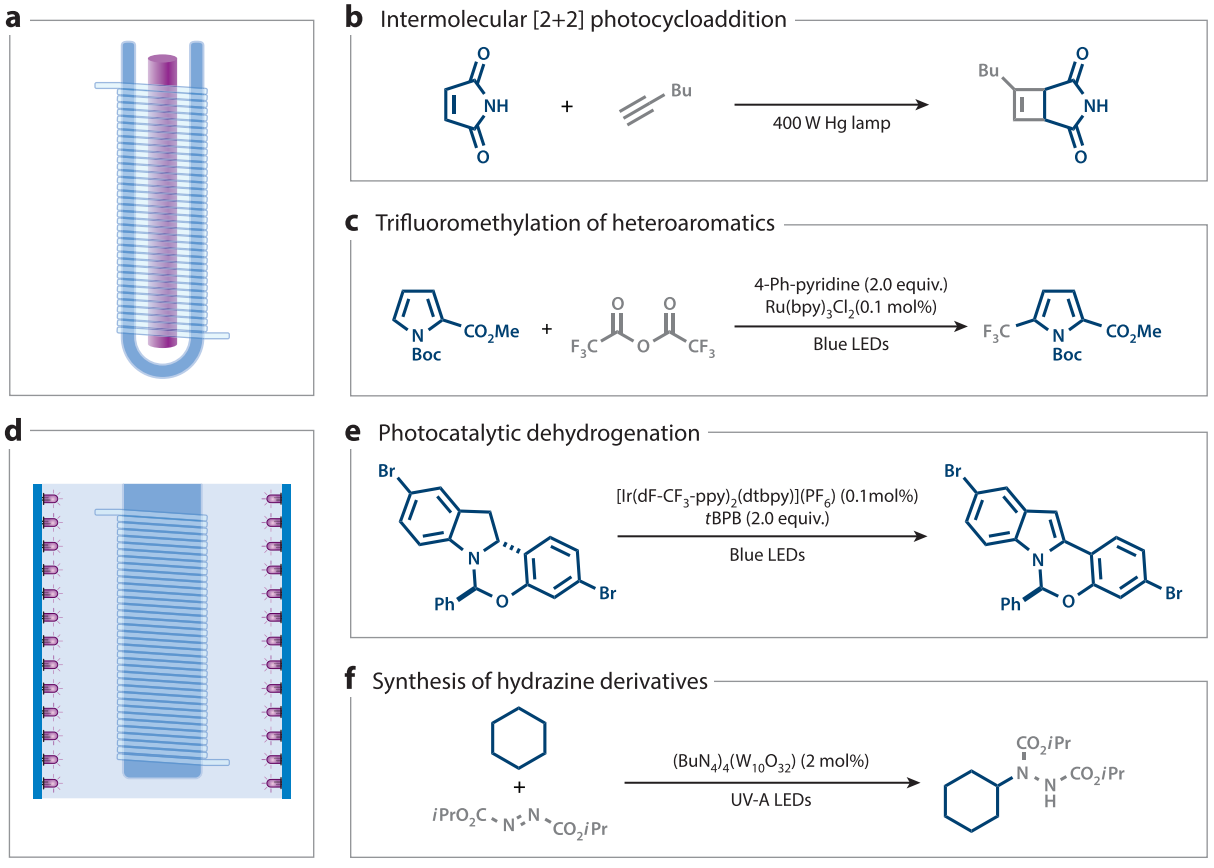

Figure 3

(*a*) Capillary flow reactor with illumination from the inside. (*b*) The [2 + 2] photocycloaddition in flow. (*c*) The trifluoromethylation in flow. (*d*) Capillary flow reactor with illumination from the outside. (*e*) The photocatalytic dehydrogenation of indoline. (*f*) The hydrogen atom transfer process for the synthesis of hydrazine derivatives in flow. Abbreviations: LED, light-emitting diode; *t*BPB: *tert*-butyl peroxybenzoate.

the emitted wavelengths, namely in the UV-B/A and visible regions. The immersion well reactor can be cooled easily by directing water through its cooling jacket, and the lamp could potentially be replaced with one of a different nature. To prove the efficiency of this design, the authors carried out a [2 + 2] photocycloaddition (**Figure 3*b***) using a medium-pressure mercury lamp (400 W) to photoexcite the maleimide reaction partner. Under the optimized reaction conditions, this design afforded the corresponding target molecule in a residence time of 26 min and a projected 24-h production of 685 g.

Stephenson and coworkers (37) used a similar design to enable a multigram scale-up of the photocatalytic perfluoroalkylation of aromatic compounds with pyridine *N*-oxides. Specifically, the authors used a set of blue light-emitting diodes (LEDs) to match with the absorption spectrum of the photocatalyst and used perfluoroalkoxy (PFA) tubing as reactor (internal volume 150 mL, ID 1.6 mm). The targeted trifluoromethylated pyrrole (**Figure 3*c***) could be obtained in a residence time of 30 min, leading to a productivity of 600 g/day.

A collaboration between the Knowles group and Merck used capillary flow technology to perform a scale-up of a light-triggered dehydrogenation of indoline for the synthesis of elbasvir (38)

(**Figure 3*e***). This reactor is characterized by blue light illumination from the outside of the PFA capillary (**Figure 3*d***). The reactor coil was wrapped around an Ace glass condenser (internal volume 150 mL, ID 3.1 mm), which was kept at a temperature below 0°C to avoid racemization of both starting material and product. Using this reactor, they obtained the targeted dehydrogenated product employing only 0.1 mol% of the iridium-based photocatalyst and 2 equivalents of *tert*-butylperbenzoate as oxidant. With a residence time of 60 min, a 24-h production of ∼500 g was projected with almost negligible erosion on the enantiopurity (99.8%ee).

All the aforementioned procedures use reactors characterized by a rather large volume (150–210 mL). More recently, a collaboration between the Noël research group and Signify has resulted in a photoreactor capable of performing reactions in a very short residence time and with reduced reactor volume due to the high photon flux provided by a powerful illumination source (optical power output 144 W) (39). This reactor design consists of a metal support coiled with PFA tubing (ID 0.7 mm) and irradiated by 6 UV-A chip-on-board LEDs, each attached to a heat dissipation element and a fan. By using this reactor, the authors carried out a photocatalytic hydrogen atom transfer procedure to convert alkane substrates into the corresponding protected hydrazine derivatives in a capillary reactor of only 11 mL with a productivity of 2.15 kg/day (40) (**Figure 3*f***).

Researchers from Merck recently showed that capillary PFR reactors can be used to support pilot-scale production (41). Hereto, a fluorinated ethylenepropylene–based tubular reactor (internal volume 830 mL, ID 7.1 mm) was coiled and housed between two glass plates, which could be cooled (**Figure 4*a***). The reactor was irradiated with high-intensity LED chips (total power

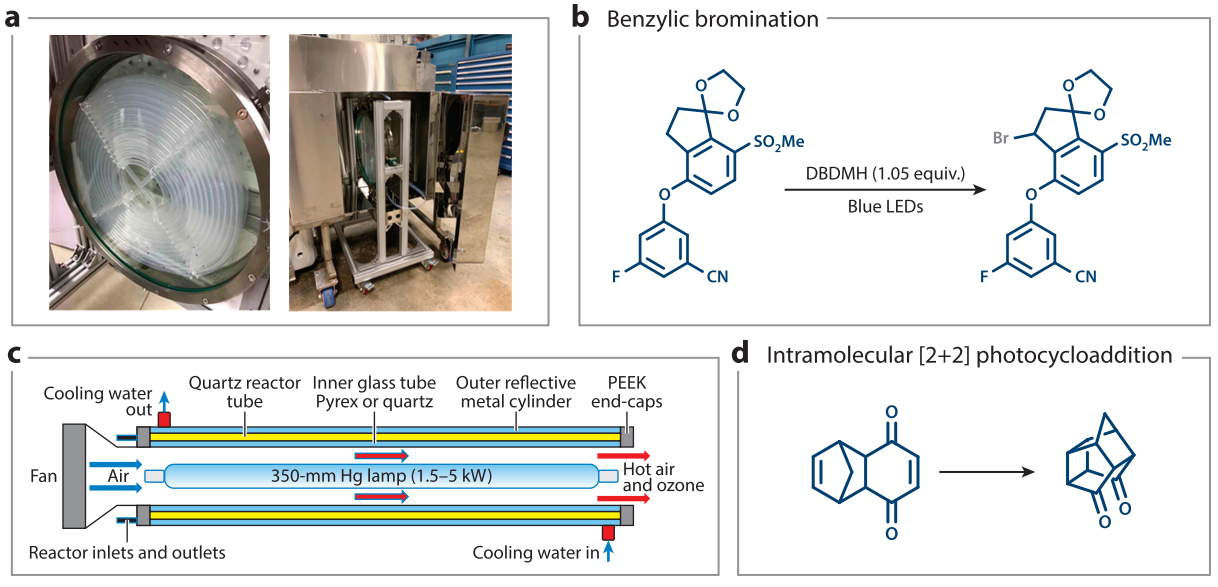

Figure 4

(*a*) The housing containing the coiled tubular reactor and this reactor placed inside the LED skid. Adapted with permission from Reference 41; copyright 2022 American Chemical Society. (*b*) Benzylic bromination in flow. (*c*) Schematic representation of the Firefly reactor. Adapted with permission from Reference 42; copyright 2016 American Chemical Society. (*d*) The intramolecular [2 + 2] photocycloaddition in flow. Abbreviations: DBDMH: 1,3-dibromo-5,5-dimethylhydantoin; LED, light-emitting diode; PEEK, polyether ether ketone.

input 800 W, LED panels were glycol cooled). This setup enabled the scaling of the benzylic photobromination of a key indane intermediate for the preparation of belzutifan (**Figure 4*b***): 50 kg of indane derivative could be converted in 32 h (1.5 min residence time, 38 kg/day productivity), yielding the target brominated compound in an assay yield of 93%.

Booker-Milburn and coauthors (42) developed another design to increase productivity in which the reaction mixture is introduced into parallel-positioned tubes. This design, also known as parallel tube flow reactor and coined the Firefly reactor (**Figure 4*c***), was conceived with the aim of producing more than one kilogram of product per day, while not increasing the overall footprint of the reactor or the size of the light source with respect to the previous capillary designs. To realize this goal, the authors decided to use more durable and UV-transparent quartz tubes (internal volume 120 mL), positioned around the central mercury lamp in a parallel fashion. The individual tubes were subsequently connected in series. Additionally, a double cooling system was integrated within the reactor to avoid overheating: The reactor tubes were encapsulated within a fluid-cooled annular cavity, and a fan was located at one of the sides of the reactor, providing additional cooling. A metal reflector was placed around the reactor to maximize the exposure of the reaction mixture to the UV light. As a result, the authors could carry out a benchmark [2 + 2] photocycloaddition (**Figure 4*d***) with a productivity of 8 kg/day.

Due to their simplicity, adaptability, and low cost, capillary microreactors are the most-used reactor type for scaling up light-promoted reactions. However, other reactor designs also have been used, such as microstructured reactors. As an example, Alcazar and coauthors (43) used a commercially available glass plate reactor, i.e., the Corning Advanced-Flow Reactor (AFR) G1, to scale the visible light–induced two-step Negishi cross-coupling process (**Figure 5*a***). This strategy consists of the light-enhanced nickel-catalyzed coupling between an aryl bromide and an organozinc reagent, which was prepared by directing an alkyl halide–containing solution over a column filled with zinc powder (**Figure 5*b***). The photochemical reactor is the result of a sizing-up approach in which five glass-based fluidic modules of 8.2 mL each were connected in series [also called numbering-up in series (21)]. To ensure proper illumination, each module was irradiated from both sides with a 405-nm LED panel. By using reaction conditions almost identical to those used on a laboratory scale (44), a seven- to tenfold increase in productivity was obtained (5.6 g/h). This enhanced throughput is due not only to a fourfold increase in the reactor volume but also to the higher light intensity, which ensures effective irradiation of the reaction mixture.

Kappe and colleagues (45) also used the Corning-type flow reactors to carry out a photochemical benzylic bromination. The process relies on the in situ generation of Br_2 in flow by reacting concentrated HBr and $NaBrO_3$, which is subsequently combined with 2,6-dichlorotoluene and introduced into the photochemical G1 Low Flow reactor (internal volume 2.5 mL) (**Figure 5*c***). The use of this type of reactor proved crucial due to its increased mixing ability: The Corning AFR G series is characterized by several heart-shaped cells containing internal obstacles that function as static mixers and improve mass transfer (**Figure 5*a***). After leaving the photochemical reactor, the reaction stream is quenched in a second G1 Low Flow reactor by a sodium thiosulfate solution, ensuring complete conversion of Br_2 and thus reducing the risks associated with handling of this hazardous compound. By using this reactor, a good projected throughput of ∼6 kg/day was obtained inside the reactor assembly with an internal volume of only 5 mL for the photochemical step. Similarly, the authors proved that by using the Corning G3 reactor (∼50 mL internal volume) under reoptimized conditions, an increased throughput of ∼96 kg/day could be realized (46).

Most of the reactors discussed so far exploit passive mixing principles; i.e., the flow energy delivered by the pumps is used to enable mixing of the reaction mixture (48, 49). Mixing behavior

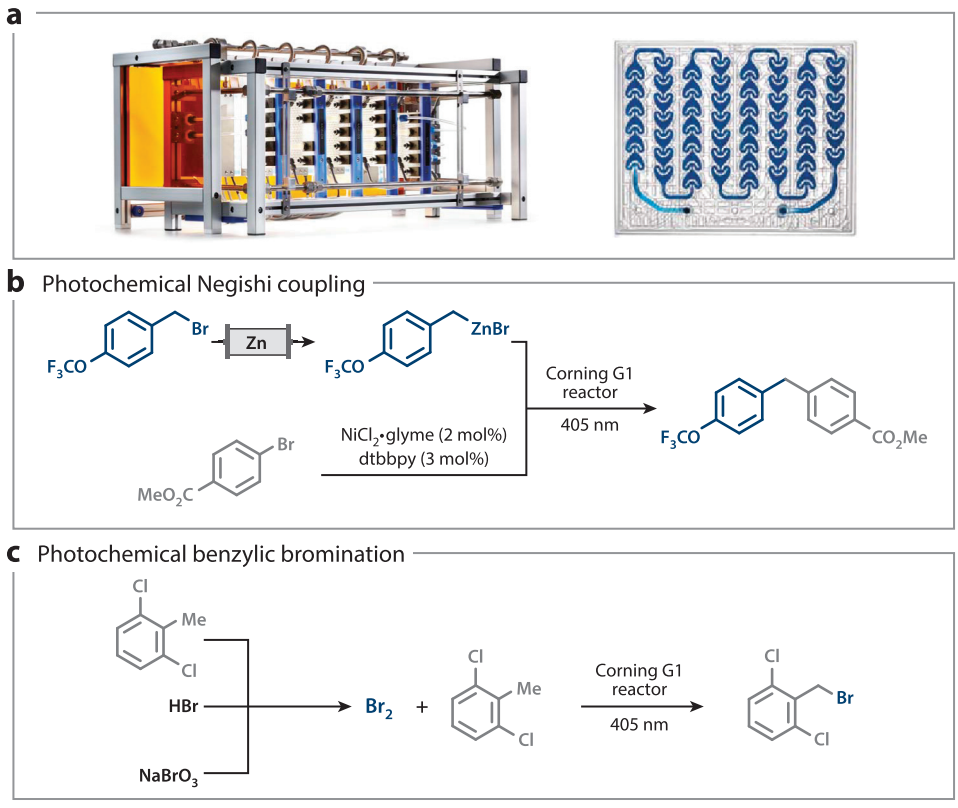

Figure 5

(*a*) The G1 photoreactor with heart-shaped fluidic modules. Adapted with permission from Reference 47; copyright 2016 Corning Inc. (*b*) The photochemical Negishi cross-coupling in flow. (*c*) The photochemical benzylic bromination in flow. Abbreviations: dtbbpy, 4,4′-di-*tert*-butyl-2,2′-dipyridyl; glyme, dimethyl glycol.

in this class is intensified by reactor orientation and shape, such as the static mixing units, sharp bends, or local constrictions. However, some reactors combine both passive and active mixing principles to intensify the mass- and heat-transfer phenomena. This is useful particularly for multiphase reaction mixtures, where mass transfer between two or more phases must be ensured. Active mixing involves the supply of additional energy to increase mixing. Examples are the use of pulsations, ultrasound energy, or mechanical stirring.

A first example involving both active and passive mixing is the HANU reactor, developed by Creaflow (**Figure 6*a***). The HANU microstructured reactor is an oscillatory flow reactor, which uses static mixing elements in combination with a pulsated flow (50). Notably, these oscillations also allow one to sustain a slurry without the occurrence of reactor clogging (51), a common issue encountered in continuous-flow capillaries (52). The reactor was benchmarked using a photocatalytic nickel-catalyzed $C(sp^2)$–$C(sp^3)$ reductive cross-coupling between methyl 4-bromobenzoate and 4-bromotetrahydropyran with Na_2CO_3 as an inorganic solid base (**Figure 6*b***). The residence time was reduced from 6 h in batch to 30 min in flow. The final productivity was 0.87 g/h, compared to only 0.014 g/h in batch. The scale-up potential of the HANU reactor was demonstrated further for a homogeneous photocatalytic $C(sp^3)$–H alkylation using TBADT (53), photocatalytic C–N cross-coupling reactions using the heterogeneous photocatalyst graphitic nitride (54), and photocatalytic atom transfer radical addition reactions (55).

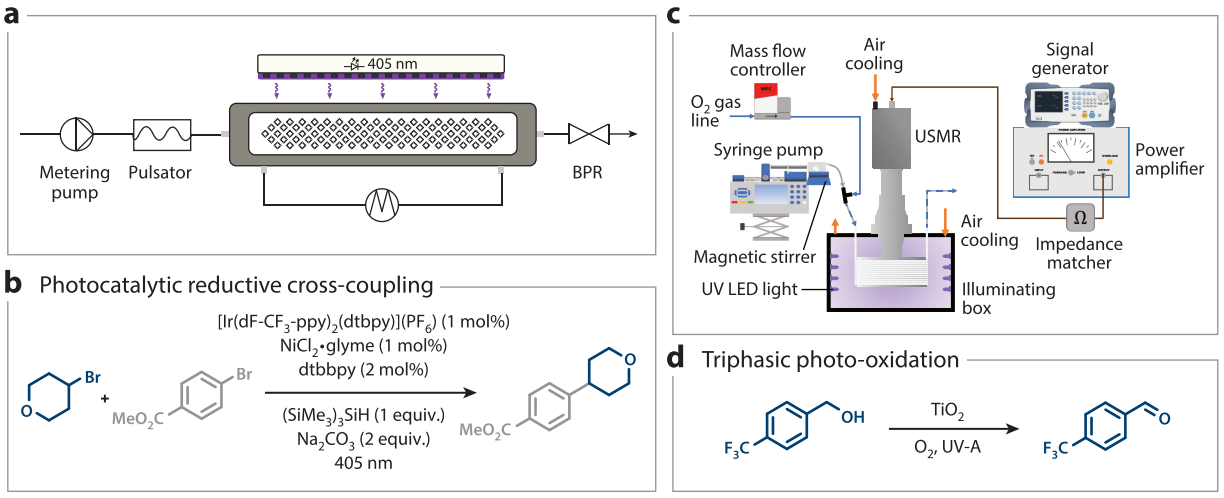

Figure 6

(*a*) Schematic representation of the HANU HX 15 reactor setup. Adapted with permission from Reference 51; copyright 2020 American Chemical Society. (*b*) The photocatalytic reductive cross-coupling in flow. (*c*) Schematic representation of the ultrasonic photochemical reactor. Adapted with permission from Reference 56; copyright 2022 Elsevier. (*d*) The triphasic photochemical photooxidation in flow. Abbreviations: BPR, back pressure regulator; dtbbpy, 4,4′-di-*tert*-butyl-2,2′-dipyridyl; glyme, dimethyl glycol; LED, light-emitting diode; USMR, ultrasonic millireactor.

Noël and colleagues (56) developed an ultrasonic (US) photochemical reactor, which was operated by simultaneous irradiation of the glass capillaries with ultrasound and visible light (**Figure 6*c***). US irradiation of reaction mixtures can cause various physical phenomena, of which cavitation bubble formation and subsequent collapse are the primary effects of interest. US irradiation can intensify mixing and break up particle agglomerations, thereby preventing clogging of capillaries and providing another method for solids handling in flow. The US reactor was custom designed and includes a transducer that generates the soundwave, which is then propagated through a sonotrode and large irradiating cylinder. This assembly is responsible for the transformation of standing waves in the longitudinal direction through the sonotrode into the radial direction of the cylinder. The glass capillary (ID 2.2 mm, 13 mL) is coiled around this cylinder, enabling the direct internal US irradiation of the reaction mixture (22.6 kHz, 60 W) while leaving the external part available for light irradiation (365-nm LEDs, 65 W input power). Despite the compressed air cooling, a large temperature rise of the reactor mixture was observed during continuous US irradiation, necessitating a shift toward pulsed on–off sonication. A triphasic photooxidation of 4-(trifluoromethyl)benzyl alcohol to the corresponding aldehyde with oxygen and the heterogeneous photocatalyst titanium dioxide (**Figure 6*d***) was performed to showcase the intensified mixing and solids-handling capabilities of the setup, resulting in a significant increase in conversion and preventing clogging.

Another classic example of active mixing is the commonly used continuous stirred-tank reactor (CSTR), in which a stirrer (e.g., magnetic, propeller) agitates the reaction mixture. In principle, CSTRs are stirred batch reactors but with an in- and outflow. The vessel itself is typically larger than the previously discussed PFRs. Researchers from AbbVie demonstrated that a photochemical CSTR platform can facilitate scaling of photochemical transformations (57). Their setup makes use of a fiber-optic laser (25 W output power, 450 nm) that irradiates a 100-mL vessel from the top through a beam expander to cover the entire top surface with light (**Figure 7*a***). Contrary to diffuse

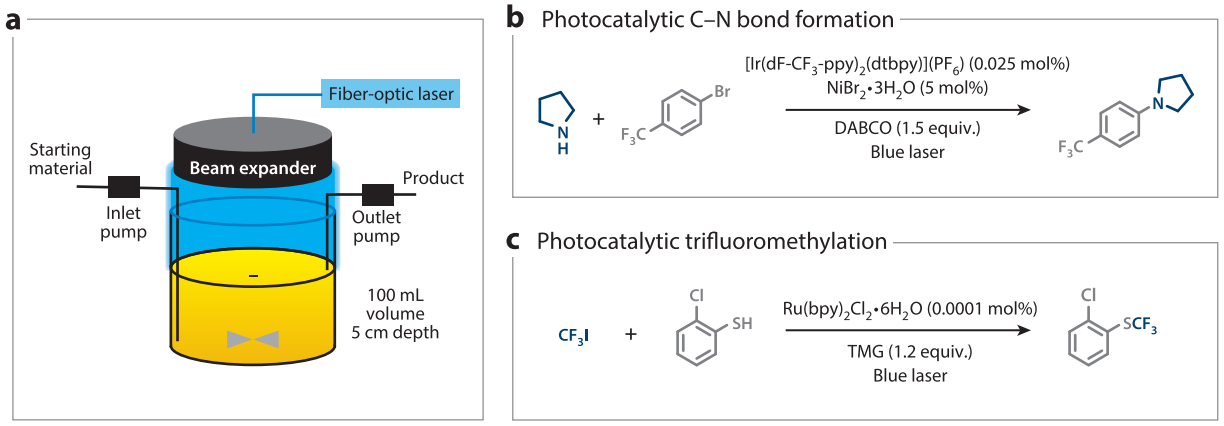

Figure 7

(*a*) Schematic representation of the laser-driven photochemical continuous stirred-tank reactor. Adapted with permission from Reference 57; copyright 2019 American Chemical Society. (*b*) The photocatalytic nickel-catalyzed C–N cross-coupling in flow. (*c*) The photocatalytic trifluoromethylation using dissolved CF_3I gas in flow. Abbreviations: DABCO, 1,4-diazabicyclo[2.2.2]octane; TMG, 1,1,3,3-tetramethylguanidine.

LED irradiation, a laser offers high-intensity focused light, allowing placement of the light source further away from the reaction mixture than is necessary for diffuse light sources. This decouples the heat generated by the light source from the reactor part and thus does not affect the internal reactor temperature. The high-power laser enables irradiation through the reactor for the entire 5-cm optical path depth in the vessel, and agitation is achieved by a magnetic stirrer positioned at the bottom of the vessel. With the inlet placement at the bottom and outlet as an overflow at the top, the RTD experiments showed almost ideal CSTR behavior. The reactor platform showcased a photocatalytic nickel-catalyzed C–N cross-coupling (**Figure 7*b***) resulting in 1.8 kg of product in 32 h, yielding a productivity of 1.2 kg/day in the 100-mL device. Next, researchers from AbbVie and Asymchem developed and demonstrated a fully continuous multistep process in which the first photochemical step, i.e., the trifluoromethylation of 2-chlorothiophenol with dissolved CF_3I gas (**Figure 7*c***), was performed in a large-scale laser-driven CSTR (1 L, 300 mL irradiated volume) (58). The fully continuous process included a consecutive oxidation of the trifluoromethylated product, intermediate washes, and settlers/separators. Performing the photochemical step in the jacketed laser-driven CSTR resulted in an overall process productivity of 50 kg/day.

The working principle of an ideal CSTR is intrinsically different from those of batch reactors or ideal PFRs. In a CSTR, the ideal mixing ensures that reagent/product concentrations are homogeneous throughout the entire reactor. In batch reactors and PFRs, the conversion of the starting material varies over time or along the reactor length, respectively. Due to this difference, CSTRs generally require a larger reactor volume than PFRs to achieve the targeted conversions. A classical method to mitigate this issue and to ensure high conversions is to connect multiple smaller-volume CSTRs in series (59), emulating the gradual change in conversion of the PFR. For their laser-driven CSTR platform, the researchers at AbbVie also theoretically envisioned this concept using a so-called Levenspiel analysis to reduce the required reactor volume in order to enhance projected productivity of the C–N cross-coupling product from 1.2 to 3.9 kg/day by operating two CSTRs (100 and 38 mL in volume) in series, with a separate laser each (57).

Jensen and coworkers (60) also exploited this CSTRs-in-series concept. The setup consists of 5 sequential mini-CSTRs, each equipped with a stirring bar (5.3 mL total reactor volume). The setup is irradiated by 3× 40-W blue LED light sources (440 nm) focused through condenser

lenses. Emulating PFR behavior with this setup has one major advantage over a PFR: Given the overall larger dimensions, the risk of clogging can be minimized. The authors demonstrated this during an extended run of 13 h, in which 1 g of the cross-coupling product between 4-bromotetrahydropyran and methyl-4-bromobenzoate (see **Figure 6*b*** for reaction scheme) could be isolated. Interestingly, the solid base was fed into the system separately from the homogeneous reaction mixture by a custom-made slurry pump.

Alternative reactor designs that are closely related to the traditional stirring methods used in CSTRs exploit high-velocity rotating structures and can achieve highly efficient mixing and high shear rates (61). These conceptually interesting reactors comprise a static part (called the stator) and a rotating part (called the rotor), and these two components are separated by a narrow gap (mostly a few millimeters). Due to fast rotation of the rotor, the fluid experiences high shear rates, and turbulence and vortices are induced in the reaction mixture, which significantly increase mass and heat transfer.

George, Poliakoff, and colleagues (62) applied this principle in the development of a so-called vortex reactor. The reactor consists of a bored stainless-steel rod suspended from the top of the reactor, serving as the rotor, and a jacketed glass tube, as the stator. The active irradiated reactor volume (8 mL) is confined in the annular space between the rotor and stator (~1 mm), which is irradiated by white LEDs. Similar to overflow CSTRs, the reaction mixture was fed from the bottom (through the bored center of the rotor) and collected at the top, which was open to air. The photocatalytic oxidation of α-terpinene to ascaridole was used as the benchmark reaction (**Figure 8*a***), where the required oxygen was drawn from the air headspace at the top of the reactor. High-velocity rotation of the rod caused local depressions, allowing the air to be drawn into the annular volume, where Taylor–Couette vortices intensified mixing and facilitated dispersion of air into the reaction mixture. Because this benchmark reaction can suffer from selectivity issues

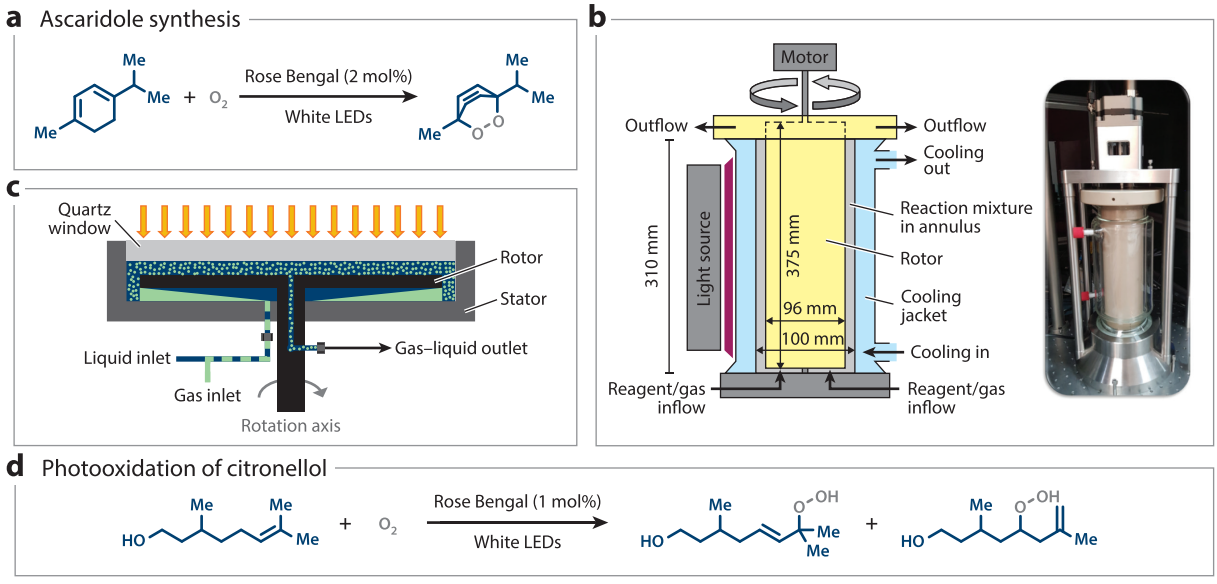

Figure 8

(*a*) The photocatalytic oxidation of α-terpinene to ascaridole in flow. (*b*) Schematic representation and picture of the scaled-up vortex reactor. Adapted with permission from Reference 63; copyright 2020 American Chemical Society. (*c*) Schematic representation of the photochemical rotor-stator spinning disk reactor. Adapted with permission from Reference 64; copyright 2020 Elsevier. (*d*) The photooxidation of β-citronellol in flow. Abbreviation: LED, light-emitting diode.

with the undesired formation of *p*-cymene, and because the uptake of oxygen in the system is highly dependent on the rotational speed, the rpm (revolutions per minute) was varied to find optimal operating conditions. At optimal conditions, a productivity of 11 g/day toward the desired ascaridole product was demonstrated.

Next, the same authors developed a scaled-up version of the vortex reactor (63) (**Figure 8*b***). This design abandoned the open-top concept, as well as the feed through the bored rod. Instead, to allow for more feed control and scale-up possibilities, an open-ended jacketed tube/cylinder was equipped with feed at the bottom, suitable for both liquid and gaseous feed, and collection of the reaction mixture at the top. The rod was replaced with a rotating cylinder (diameter of 96 mm versus 18 mm in the first generation), which requires overall lower rotational speeds to generate comparable hydrodynamic behavior in the annular volume. This significantly larger vortex reactor (2-mm gap, 280-mL annular volume) can be irradiated by LED blocks or medium-pressure mercury lamps for visible-light or UV purposes, respectively. The (visible-light) photooxidation of β-citronellol using pure oxygen was used as a benchmark for comparison between the two generations (**Figure 8*d***). Less than 10 g/day of product was achieved in the first generation, whereas the productivity for the second generation exceeded 1.6 kg/day. A projected productivity of 7.5 kg/day for the (UV-irradiated) [2 + 2] photocycloaddition of a tricyclic dione to its corresponding diketone was also reported (see reaction scheme in **Figure 4*b***).

Another example of active mixing that exploits the rotor-stator concept is the photochemical rotor-stator spinning disk reactor (pRS-SDR) developed by Noël, van der Schaaf, and colleagues (64). This reactor concept consists of a cylindrical stator with a rotating disk as rotor. The axis of the disk is connected solely at the bottom, leaving the flat top surface of the disk available to be irradiated through the quartz top window (**Figure 8*c***). The gas–liquid reaction feed is introduced at the bottom of the stator, and the outlet is positioned in the center of the disk's top surface, escaping through the axis of the rotor. The high shear rates created by the rotational speed effectively disperse the co-fed gas into the liquid phase: The average gas bubble size reduces with increasing rpm, resulting in a higher interfacial area. Interestingly, just as the theoretical average residence time in a CSTR is not influenced by its stirring speed, the residence time of the pRS-SDR is independent of the rotational speed of the disk. This effectively decouples the mixing and the hydrodynamic behavior from the used flow rates, allowing for excellent performance tuning. The setup is irradiated through the quartz window, which resulted in an irradiated volume of 27 mL (∼2-mm gap) out of the full 64-mL internal reactor volume. This is due to the nonirradiated volume below the disk. The photooxidation of α-terpinene to ascaridole was used as a benchmark reaction (see **Figure 8*a***), using high-power white LEDs. Increasing the rotational speed significantly improved reaction selectivity and yield: The pRS-SDR achieved a productivity of 1.1 kg/day at 2,000 rpm. Notably, this would require 71 capillary microreactors in parallel to match the pRS-SDR productivity. Although supply of additional mechanical energy is required to reach high rpm in these mechanically stirred reactors, it represents only 10% of the total energy input in the pRS-SDR. In other words, the light source remains the strongest contributor to the total energy balance and represents the most expensive aspect in scaling photochemical transformations. As this example shows, increasing the rotational speed strongly impacted the yield and selectivity. Thus, it seems reasonable and economically wise to use active mixers to enable process intensification in photochemical transformations.

The pRS-SDR was subsequently evaluated in a solids-containing heterogeneous photochemical transformation, as a demonstration of its ability to process slurries (65). The benchmark reaction was the aerobic photodegradation of aqueous methylene blue using titanium dioxide as a solid photocatalyst. Because this transformation is performed with UV irradiation, the light source was changed to a UV floodlight (365 nm, 175 W maximum input power). The productivity of the

pRS-SDR was compared in terms of volumetric processing rate to other reported setups and surpassed these. Due to the high shear on the reaction mixture, issues related to clogging, particle agglomeration, or settling were not observed.

SUMMARY AND FUTURE OUTLOOK

Reactions that involve photons as energy carriers have long been thought to be unscalable. Consequently, photochemistry has been mostly avoided in the chemical industry, and thus limited or no expertise has been built up to handle such transformations. However, due to the popularity of photocatalysis in the past two decades and the decisive benefits it brings along for the preparation of medicines, agrochemicals, and other chemical building blocks, research activity concerning scale-up of photochemical transformations has grown significantly.

Herein, we have shown that continuous-flow reactors are the solution to scaling photochemical transformations in both academia and industry. Successful scaling of photochemistry entails a careful balance between a suitable light source, a proper continuous-flow reactor design, and careful reaction engineering. Depending on the reaction scale and the nature of the reaction mixture, various reactor types can be used in combination with additional active or passive mixing elements. Furthermore, although a single reactor might not be sufficient, a combination of numbering up and sizing up should enable process engineers to meet the production targets.

Although substantial reaction scales can be accessed nowadays, more work remains. Solving the remaining issues will require a concerted effort from chemists, chemical engineers, and light developers.

A first issue involves the development of cheaper and more energy-efficient light sources, especially in the UV-B and -C region where no suitable LEDs are yet available. Although for visible light and UV-A excellent LED solutions with long lifetimes and good energy efficiency are on the market, the cost of photons remains high. Hence, more efficient use of these photons is needed, e.g., through the development of photochemical transformations that rely on radical chains (i.e., a single photon leads to many product molecules) and through better reactor design that reflects nonabsorbed photons. Alternatively, solar light could be harvested as a free and sustainable energy source. Notably, some specially designed reactors have been developed recently that can exploit solar energy to drive photocatalytic transformations (66, 67).

Second, the combination of mass-, heat-, and photon-transport phenomena is undoubtedly challenging, and thus more effective models, relations, and correlations are required to help researchers understand and predict the overall photochemical reaction process. As more fundamental knowledge is built up, researchers in the chemical industry will become more confident in implementing photochemical steps in their synthetic routes.

Third, standardized reactor units are required to ensure widespread implementation of photochemistry. As shown here, most companies develop internally customized scaled-up reactor solutions for their photocatalytic transformations. Therefore, off-the-shelf reactor units with suitable and fully characterized light sources would be of high interest. Due to the continued efforts of researchers in both academia and industry to streamline the scaling of photochemical transformations, we anticipate that the use of such activation modes will become mainstream in the chemical industry.

DISCLOSURE STATEMENT

The authors are not aware of any affiliations, memberships, funding, or financial holdings that might be perceived as affecting the objectivity of this review.

ACKNOWLEDGMENTS

S.D.A.Z., D.M., and T.N. would like to thank the European Union's Horizon 2020 research and innovation program for generous research funding (FlowPhotoChem, no. 862453, S.D.A.Z., T.N.; ELECTRORGANO, no. 101022144, D.M.).

LITERATURE CITED

1. Melchiorre P. 2022. Introduction: photochemical catalytic processes. *Chem. Rev.* 122(2):1483–84
2. Balzani V, Ceroni P, Juris A. 2014. *Photochemistry and Photophysics: Concepts, Research, Applications*. Hoboken, NJ: John Wiley & Sons
3. Turro NJ, Ramamurthy V, Scaiano JC. 2010. *Modern Molecular Photochemistry of Organic Molecules*. Sausalito, CA: Univ. Sci. Books
4. Albini A, Fagnoni M. 2013. *Photochemically-Generated Intermediates in Synthesis*. Hoboken, NJ: John Wiley & Sons
5. Kärkäs MD, Porco JA, Stephenson CRJ. 2016. Photochemical approaches to complex chemotypes: applications in natural product synthesis. *Chem. Rev.* 116(17):9683–747
6. Kavarnos GJ. 1993. *Fundamentals of Photoinduced Electron Transfer*. Weinheim, Ger.: VCH Publ.
7. Strieth-Kalthoff F, James MJ, Teders M, Pitzer L, Glorius F. 2018. Energy transfer catalysis mediated by visible light: principles, applications, directions. *Chem. Soc. Rev.* 47(19):7190–202
8. Capaldo L, Ravelli D, Fagnoni M. 2022. Direct photocatalyzed hydrogen atom transfer (HAT) for aliphatic C-H bonds elaboration. *Chem. Rev.* 122(2):1875–924
9. Stephenson CRJ, Studer A, Curran DP. 2013. The renaissance of organic radical chemistry—deja vu all over again. *Beilstein J. Org. Chem.* 9:2778–80
10. Anastas PT, Warner JC. 1998. *Green Chemistry: Theory and Practice*. New York: Oxford Univ. Press
11. Yoon TP, Ischay MA, Du J. 2010. Visible light photocatalysis as a greener approach to photochemical synthesis. *Nat. Chem.* 2(7):527–32
12. Crisenza GEM, Melchiorre P. 2020. Chemistry glows green with photoredox catalysis. *Nat. Commun.* 11:803
13. Noël T, Zysman-Colman E. 2022. The promise and pitfalls of photocatalysis for organic synthesis. *Chem. Catal.* 2(3):468–76
14. Buglioni L, Raymenants F, Slattery A, Zondag SDA, Noël T. 2022. Technological innovations in photochemistry for organic synthesis: flow chemistry, high-throughput experimentation, scale-up, and photoelectrochemistry. *Chem. Rev.* 122(2):2752–906
15. Darvas F, Hessel V, Dorman G, eds. 2014. *Flow Chemistry—Fundamentals*. Berlin: De Gruyter
16. Gavriilidis A, Constantinou A, Hellgardt K, Hii KK(M), Hutchings GJ, et al. 2016. Aerobic oxidations in flow: opportunities for the fine chemicals and pharmaceuticals industries. *React. Chem. Eng.* 1(6):595–612
17. Burange AS, Osman SM, Luque R. 2022. Understanding flow chemistry for the production of active pharmaceutical ingredients. *iScience* 25(3):103892
18. Holtze C, Boehling R. 2022. Batch or flow chemistry?—A current industrial opinion on process selection. *Curr. Opin. Chem. Eng.* 36:100798
19. Jensen KF. 2017. Flow chemistry—Microreaction technology comes of age. *AIChE J.* 63(3):858–69
20. Rogers L, Jensen KF. 2019. Continuous manufacturing—the Green Chemistry promise? *Green Chem.* 21(13):3481–98
21. Dong Z, Wen Z, Zhao F, Kuhn S, Noël T. 2021. Scale-up of micro- and milli-reactors: an overview of strategies, design principles and applications. *Chem. Eng. Sci. X* 10:100097
22. Berton M, de Souza JM, Abdiaj I, McQuade DT, Snead DR. 2020. Scaling continuous API synthesis from milligram to kilogram: extending the enabling benefits of micro to the plant. *J. Flow Chem.* 10(1):73–92
23. Zhang J, Wang K, Teixeira AR, Jensen KF, Luo G. 2017. Design and scaling up of microchemical systems: a review. *Annu. Rev. Chem. Biomol. Eng.* 8:285–305
24. Kuijpers KPL, van Dijk MAH, Rumeur QG, Hessel V, Su Y, Noël T. 2017. A sensitivity analysis of a numbered-up photomicroreactor system. *React. Chem. Eng.* 2(2):109–15

25. Bonfield HE, Knauber T, Lévesque F, Moschetta EG, Susanne F, Edwards LJ. 2020. Photons as a 21st century reagent. *Nat. Commun.* 11:804
26. Aillet T, Loubiere K, Dechy-Cabaret O, Prat L. 2014. Accurate measurement of the photon flux received inside two continuous flow microphotoreactors by actinometry. *Int. J. Chem. React. Eng.* 12(1):257–69
27. Studer A, Curran DP. 2016. Catalysis of radical reactions: a radical chemistry perspective. *Angew. Chem. Int. Ed.* 55(1):58–102
28. Cismesia MA, Yoon TP. 2015. Characterizing chain processes in visible light photoredox catalysis. *Chem. Sci.* 6(10):5426–34
29. Buzzetti L, Crisenza GEM, Melchiorre P. 2019. Mechanistic studies in photocatalysis. *Angew. Chem. Int. Ed.* 58(12):3730–47
30. Corcoran EB, McMullen JP, Lévesque F, Wismer MK, Naber JR. 2020. Photon equivalents as a parameter for scaling photoredox reactions in flow: translation of photocatalytic C–N cross-coupling from lab scale to multikilogram scale. *Angew. Chem. Int. Ed.* 59(29):11964–68
31. Bloh JZ. 2019. A holistic approach to model the kinetics of photocatalytic reactions. *Front. Chem.* 7:128
32. Donnelly K, Baumann M. 2021. Scalability of photochemical reactions in continuous flow mode. *J. Flow Chem.* 11(3):223–41
33. Di Filippo M, Bracken C, Baumann M. 2020. Continuous flow photochemistry for the preparation of bioactive molecules. *Molecules* 25(2):356
34. Kayahan E, Jacobs M, Braeken L, Thomassen LCJ, Kuhn S, et al. 2020. Dawn of a new era in industrial photochemistry: the scale-up of micro: the mesostructured photoreactors. *Beilstein J. Org. Chem.* 16:2484–504
35. Noël T. 2017. *Photochemical Processes in Continuous-Flow Reactors: From Engineering Principles to Chemical Applications*. London: World Sci.
36. Hook BDA, Dohle W, Hirst PR, Pickworth M, Berry MB, Booker-Milburn KI. 2005. A practical flow reactor for continuous organic photochemistry. *J. Org. Chem.* 70(19):7558–64
37. Beatty JW, Douglas JJ, Miller R, McAtee RC, Cole KP, Stephenson CRJJ. 2016. Photochemical perfluoroalkylation with pyridine *N*-oxides: mechanistic insights and performance on a kilogram scale. *Chemistry* 1(3):456–72
38. Yayla HG, Peng F, Mangion IK, McLaughlin M, Campeau L-C, et al. 2016. Discovery and mechanistic study of a photocatalytic indoline dehydrogenation for the synthesis of elbasvir. *Chem. Sci.* 7(3):2066–73
39. Mazzarella D, Pulcinella A, Bovy L, Broersma R, Noël T. 2021. Rapid and direct photocatalytic C(sp^3)–H acylation and arylation in flow. *Angew. Chem. Int. Ed.* 60(39):21277–82
40. Wan T, Wen Z, Laudadio G, Capaldo L, Lammers R, et al. 2022. Accelerated and scalable C(sp^3)-H amination via decatungstate photocatalysis using a flow photoreactor equipped with high-intensity LEDs. *ACS Cent. Sci.* 8(1):51–56
41. Bottecchia C, Lévesque F, McMullen JP, Ji Y, Reibarkh M, et al. 2022. Manufacturing process development for belzutifan, part 2: a continuous flow visible-light-induced benzylic bromination. *Org. Process Res. Dev.* 26(3):516–24
42. Elliott LD, Berry M, Harji B, Klauber D, Leonard J, Booker-Milburn KI. 2016. A small-footprint, high-capacity flow reactor for UV photochemical synthesis on the kilogram scale. *Org. Process Res. Dev.* 20(10):1806–11
43. Abdiaj I, Horn CR, Alcazar J. 2019. Scalability of visible-light-induced nickel Negishi reactions: a combination of flow photochemistry, use of solid reagents, and in-line NMR monitoring. *J. Org. Chem.* 84(8):4748–53
44. Abdiaj I, Fontana A, Gomez MV, de la Hoz A, Alcázar J. 2018. Visible-light-induced nickel-catalyzed Negishi cross-couplings by exogenous-photosensitizer-free photocatalysis. *Angew. Chem. Int. Ed.* 57(28):8473–77
45. Steiner A, Williams JD, de Frutos O, Rincón JA, Mateos C, Kappe CO. 2020. Continuous photochemical benzylic bromination using *in situ* generated Br_2: process intensification towards optimal PMI and throughput. *Green Chem.* 22(2):448–54
46. Steiner A, Roth PMC, Strauss FJ, Gauron G, Tekautz G, et al. 2020. Multikilogram per hour continuous photochemical benzylic brominations applying a smart dimensioning scale-up strategy. *Org. Process Res. Dev.* 24(10):2208–16

47. Corning. 2022. *Advanced-Flow™ Reactors: flipping the chemical engineering world upside down.* **https://www.corning.com/emea/en/innovation/corning-emerging-innovations/advanced-flow-reactors.html**
48. Hessel V, Löwe H, Schönfeld F. 2005. Micromixers—a review on passive and active mixing principles. *Chem. Eng. Sci.* 60(8–9):2479–501
49. Green J, Holdø A, Khan A. 2007. A review of passive and active mixing systems in microfluidic devices. *Int. J. Multiphys.* 1(1):1–32
50. Bianchi P, Williams JD, Kappe CO. 2020. Oscillatory flow reactors for synthetic chemistry applications. *J. Flow Chem.* 10(3):475–90
51. Debrouwer W, Kimpe W, Dangreau R, Huvaere K, Gemoets HPL, et al. 2020. Ir/Ni photoredox dual catalysis with heterogeneous base enabled by an oscillatory plug flow photoreactor. *Org. Process Res. Dev.* 24(10):2319–25
52. Hartman RL. 2012. Managing solids in microreactors for the upstream continuous processing of fine chemicals. *Org. Process Res. Dev.* 16(5):870–87
53. Wen Z, Maheshwari A, Sambiagio C, Deng Y, Laudadio G, et al. 2020. Optimization of a decatungstate-catalyzed C(sp^3)-H alkylation using a continuous oscillatory millistructured photoreactor. *Org. Process Res. Dev.* 24(10):2356–61
54. Rosso C, Gisbertz S, Williams JD, Gemoets HPL, Debrouwer W, et al. 2020. An oscillatory plug flow photoreactor facilitates semi-heterogeneous dual nickel/carbon nitride photocatalytic C-N couplings. *React. Chem. Eng.* 5(3):597–604
55. Bianchi P, Williams JD, Kappe CO. 2021. Continuous flow processing of bismuth-photocatalyzed atom transfer radical addition reactions using an oscillatory flow reactor. *Green Chem.* 23(7):2685–93
56. Dong Z, Zondag SDA, Schmid M, Wen Z, Noël T. 2022. A meso-scale ultrasonic milli-reactor enables gas-liquid-solid photocatalytic reactions in flow. *Chem. Eng. J.* 428:130968
57. Harper KC, Moschetta EG, Bordawekar SV, Wittenberger SJ. 2019. A laser driven flow chemistry platform for scaling photochemical reactions with visible light. *ACS Cent. Sci.* 5(1):109–15
58. Harper KC, Zhang E-X, Liu Z, Grieme T, Towne TB, et al. 2022. Commercial-scale visible light trifluoromethylation of 2-chlorothiophenol using CF_3I gas. *Org. Process Res. Dev.* 26(2):404–12
59. Hu C. 2021. Reactor design and selection for effective continuous manufacturing of pharmaceuticals. *J. Flow Chem.* 11(3):243–63
60. Pomberger A, Mo Y, Nandiwale KY, Schultz VL, Duvadie R, et al. 2019. A continuous stirred-tank reactor (CSTR) cascade for handling solid-containing photochemical reactions. *Org. Process Res. Dev.* 23(12):2699–706
61. Visscher F, van der Schaaf J, Nijhuis TA, Schouten JC. 2013. Rotating reactors—a review. *Chem. Eng. Res. Des.* 91(10):1923–40
62. Lee DS, Amara Z, Clark CA, Xu Z, Kakimpa B, et al. 2017. Continuous photo-oxidation in a vortex reactor: efficient operations using air drawn from the laboratory. *Org. Process Res. Dev.* 21(7):1042–50
63. Lee DS, Sharabi M, Jefferson-Loveday R, Pickering SJ, Poliakoff M, George MW. 2020. Scalable continuous vortex reactor for gram to kilo scale for UV and visible photochemistry. *Org. Process Res. Dev.* 24(2):201–6
64. Chaudhuri A, Kuijpers KPL, Hendrix RBJ, Shivaprasad P, Hacking JA, et al. 2020. Process intensification of a photochemical oxidation reaction using a rotor-stator spinning disk reactor: a strategy for scale up. *Chem. Eng. J.* 400:125875
65. Chaudhuri A, Zondag SDA, Schuurmans JHA, van der Schaaf J, Noël T. 2022. Scale-up of a heterogeneous photocatalytic degradation using a photochemical rotor-stator spinning disk reactor. *Org. Process Res. Dev.* 26(4):1279–88
66. Zondag SDA, Masson TM, Debije MG, Noël T. 2022. The development of luminescent solar concentrator-based photomicroreactors: a cheap reactor enabling efficient solar-powered photochemistry. *Photochem. Photobiol. Sci.* 21(5):705–17
67. Masson TM, Zondag SDA, Kuijpers KPL, Cambié D, Debije MG, Noël T. 2021. Development of an off-grid solar-powered autonomous chemical mini-plant for producing fine chemicals. *ChemSusChem* 14(24):5417–23